METHODS AND CODES FOR RESERVOIR–ATMOSPHERE ^{14}C AGE OFFSET CALCULATIONS

Guillaume SOULET[1,*]

1 Woods Hole Oceanographic Institution, Geology and Geophysics department, 266 Woods Hole Road, Woods Hole, MA-02543, USA

*corresponding author: gsoulet@whoi.edu

Abstract

Reservoir age ^{14}C offsets are invaluable tracers for past changes in carbon cycle and oceanic circulation. Reconstruction of reservoir age offsets with time is also required for calibration purposes (reconstruction of atmospheric calibration curve, calibration of non-atmospheric radiocarbon ages). Thus, properly propagating the various uncertainties linked to reservoir age offset is important for proper interpretation. However, approaches for reservoir age offset calculation – especially when considering pairs of reservoir-derived ^{14}C and calendar ages – are usually not detailed and inadequate for proper propagation of uncertainties. Here, the various ways to properly calculate reservoir age offsets are described with an emphasis on a new approach when considering pairs of ^{14}C and calendar ages. This approach maps the calendar age distribution onto the ^{14}C time scale prior to reservoir age offset calculation – the "*uncalibration-convolution process*". R codes computing reservoir age offsets based on available data are presented. Finally, a case study focusing on the reconstruction of the speleothem-atmosphere ^{14}C age offsets of speleothem ^{14}C data used in the latest release of the atmospheric calibration curve is discussed.

Keywords: Reservoir age, reservoir effect, dead carbon fraction, radiocarbon modelling, calibration curve, uncalibration process

1. Introduction

Reservoir age offset is a fundamental metric to study the dynamics of carbon exchanges between the Earth's reservoirs and attendant impacts on past climate changes. It is also widely used in geochronology calibration purposes. Whereas reservoir-atmospheric ^{14}C age offsets arise from various natural and anthropogenic processes (for a review, see Jull et al., 2013), they always derive from a $^{14}C/^{12}C$ disequilibrium between the considered carbon reservoir (e.g. surface or deep ocean, freshwater systems, soil) and the contemporaneous atmosphere (i.e. the atmospheric carbon reservoir). From a ^{14}C age point of view, this can be expressed as:

$$d^{14}R(\theta) = \rho_{res}(\theta) - \rho_{atm}(\theta) \quad (1)$$

Equation **(1)** indicates that the reservoir age offset is the deviation $d^{14}R$ between the ^{14}C age of the considered carbon reservoir ρ_{res} and the ^{14}C age of the contemporaneous atmospheric carbon reservoir ρ_{atm} at a given calendar time θ. Therefore, an either perfect or imperfect estimate of the calendar age θ needs to be available in order to derive the reservoir age offset. Note that the atmospheric carbon reservoir is used as the reference when computing the reservoir age offset, as it is the sole carbon reservoir in which ^{14}C is renewed and spatially uniform besides some second order differences between hemispheres (Hogg et al., 2013). In addition, the atmospheric ^{14}C concentration is quite precisely known for the past 14,000 calendar years and reasonably well known back to 50,000 calendar years ago (Reimer et al., 2013). Consequently, it is possible to reconstruct reservoir age offsets for calendar ages back to year 50,000 before the present (i.e., years before AD 1950; thereafter cal. a. BP). Moreover, equation **(1)** indicates that the reservoir age offset must be quoted in "^{14}C years".

Calculating reservoir age offsets seems straightforward. However, sometimes the calendar age θ is necessarily weakly known, i.e. that an uncertainty is associated to it. Indeed it may have been

obtained through scientific measurements [e.g. U/Th dating (e.g. Druffel et al., 2008; Hall et al., 2010; Southon et al., 2012) or tuning processes with calendrically-dated series of reference (e.g. Heaton et al., 2013; Soulet et al., 2011a; Thornalley et al., 2011)]. In that case, mapping the calendar age distribution onto the radiocarbon time scale (hereafter called "uncalibration") is required in order to get access to the atmospheric ^{14}C age corresponding to the calendar age $\theta \pm \sigma_\theta$. The "uncalibrating" approach is sometimes vaguely detailed in the literature, e.g., Reimer et al. (2013) wrote: "*reservoir ages were calculated from the ^{14}C difference of the overlap with the tree rings*". After the "uncalibration" step, some authors propagated uncertainties on the ^{14}C reservoir age offset through the use of the quadratic sum (e.g. Hall et al., 2010). Even though this method produces an estimate of the reservoir age offset, it turns out to be distributed according to a Gaussian distribution, since the approach neglects the structures of the atmospheric calibration curve. When the atmospheric ^{14}C wiggles are taken into account, the estimates of both "uncalibrated" ages and the resulting reservoir age offsets can be distributed according to multi-modal and asymmetric probability distributions.

Properly propagating the various uncertainties linked to reservoir age offset may help for their proper use and interpretation. This paper is intended to describe the various ways to calculate reservoir age offsets with a focus on a Bayesian approach – the "*uncalibration-convolution process*" – which properly propagates uncertainties linked to the reservoir-derived ^{14}C age, a weakly *a priori* known calendar age and the atmospheric calibration curve. A case study discusses the speleothem-atmosphere ^{14}C age offsets of speleothem ^{14}C data used in the latest release of the atmospheric calibration curve. Free and open-source codes for proper reservoir age offset calculations are provided.

2. Reservoir age offset calculations and open-source codes

According to equation **(1)**, both the ^{14}C age of the considered reservoir (e.g. ocean, a lake, a soil) and the ^{14}C age of the atmosphere in the calendar year θ have to be known to calculate the reservoir age offset. Furthermore, whatever the information we have about calendar year θ – perfectly known, weakly known or not known *a priori* – we must be certain that it corresponds to the same event Y at which reservoir/atmosphere-derived objects ceased to incorporate carbon. Hence, equation **(1)** can be written slightly differently:

$$d^{14}R(Y) = \rho_{res}(Y) - \rho_{atm}(Y) \quad (2)$$

which says that the reservoir age offset at the calendar year θ of event Y [$d^{14}R(Y)$] is equal to the difference between ^{14}C ages of the considered reservoir-derived and atmosphere-derived objects that ceased to incorporate carbon at the calendar year θ of event Y ($\rho_{res}(Y)$ and $\rho_{atm}(Y)$, respectively). From that statement, three cases of study are possible.

2.1. Reservoir age offset calculation based on a pair of ^{14}C ages

In that specific case both ^{14}C ages derived from the considered reservoir $\rho_{res}(Y) \pm \sigma_{\rho_{res}(Y)}$ and from the contemporaneous atmosphere $\rho_{atm}(Y) \pm \sigma_{\rho_{atm}(Y)}$ are *a priori* known, whereas the calendar year θ, corresponding to event Y, is unknown. The ^{14}C reservoir age offset $d^{14}R(Y)$ is easily calculated according equation **(2)**, and resulting uncertainty is given by:

$$\sigma_{d^{14}R(Y)} = \sqrt{\sigma^2_{\rho_{res}(Y)} + \sigma^2_{\rho_{atm}(Y)}} \quad (3)$$

Finally, the calendar year θ at which event Y occurred can be obtained by calibrating the atmosphere-derived ^{14}C age $\rho_{atm}(Y) \pm \sigma_{\rho_{atm}(Y)}$ using the atmospheric calibration curve (e.g., Reimer et al., 2013).

As an example, Bondevik et al. (1999) studied a sediment archive recovered on the coast of the Norwegian Sea western Norway. In the slice of sediment (609-611 cm from core top), authors found an articulated shell of *Mytilus edulis* and an assemblage of fragile terrestrial plant material. Here, the sediment slice represents the event Y corresponding to the sediment deposition of *a priori* unknown calendar year θ. The ^{14}C ages of the articulated shell and of the terrestrial plant material reflect the ^{14}C ages derived from the reservoir (coastal Norwegian Sea; $\rho_{Norvegian\ Sea}(Y) = 11565 \pm 45$ ^{14}C yr BP) and of the contemporaneous atmosphere ($\rho_{atm}(Y) = 11065 \pm 60$ ^{14}C yr BP), respectively. According to equation (2) and (3), at the calendar time of the sediment layer deposition (event Y), the ^{14}C reservoir age offset in the costal Norwegian Sea was $d^{14}R_{Norwegian\ sea}(Y) = 500 \pm 75$ ^{14}C years. Finally calibrating the atmosphere-derived ^{14}C age using Intcal13 calibration curve provides the calendar age of event Y: $\theta = 12925 \pm 70$ cal. a. BP.

However, in this approach both samples are mutually allochtonous. In other words, the terrestrial plant material has been inevitably transported before being embedded with the shell in the sediment. Thus, it is certain that the plant material ceased to incorporated radiocarbon at an event Y^* which occurred earlier than event Y reflecting the sediment deposition. Thus, the calculated ^{14}C reservoir age offset is a more or less faithful estimation of the actual one depending on the fact that event Y^* is close or not (through calendar time) to event Y. Nevertheless, by carefully selecting the dated atmospheric and reservoir-derived objects (fragile well preserved leaves, and

articulated shells for example), it might be possible to obtain a close estimation of the actual ^{14}C reservoir age offset value (e.g. Bondevik et al., 1999, 2006).

Another way to proceed is to take advantage of the virtually instantaneous deposition of volcanic ash (tephra), over wide onshore and offshore areas. In such cases, the eruption and associated tephra deposition in a sedimentary environment represent event Y. If it has been possible to determine from which eruption the tephra has been generated (usually owing to geochemical measurements carried on the tephra shards), and meaning the fact that this specific eruption has been ^{14}C-dated onshore using terrestrial remains, thus the atmosphere-derived ^{14}C age of event Y is known. Then, measuring the ^{14}C age of some material that formed in the reservoir and retrieved in the tephra layer (e.g. foraminifera for oceanic sediment cores) makes it possible to calculate the reservoir age offset. This technique is now more commonly used (e.g. Kwiecien et al., 2008; Siani et al., 2001, 2013; Southon et al., 2013) but has some limitations mainly linked to stratigraphic uncertainties (e.g. bioturbation processes; see Ascough et al., 2005; Bard et al., 1994).

Note that equation (3) applies when paired ^{14}C dates are assumed to be synchronous. However, when dealing with multiple pairs from the same sediment layer, often the case in archeological contexts, the synchronous assumption may not apply. As such, more sophisticated approaches involving Markov chain Monte Carlo sampling are required to explicitly incorporate uncertainty in the temporal relationships among paired samples (Jones and Nicholls, 2001; Jones et al., 2007; Bronk Ramsey, 2008, 2009a).

2.2. Reservoir age offset calculation based on a pair of ^{14}C age and perfectly known calendar age

Another approach is to know *a priori* the actual calendar age θ of event Y and to use the atmospheric calibration curve to derive the corresponding atmospheric ^{14}C age. This is particularly easy when dealing with pre-bomb and historical samples, i.e. for samples for which there is no uncertainty on θ.

For example, Siani et al. (2000) analyzed a mollusk shell from the collection of a museum. This mollusk was alive when it had been sampled (i.e. event Y) in the Black Sea (i.e. the reservoir) in 50 BP [i.e. *anno domini* AD 1900]. There is no uncertainty associated to θ. This mollusk yielded a radiocarbon age $\rho_{Black\ Sea}(Y)$ of 545±40 ^{14}C yrs BP. In the calendar year 50 cal. BP, the Intcal13 atmospheric calibration curve gives a ^{14}C age (i.e. $\rho_{atm}(Y)$) of 71±7 ^{14}C year BP. According to equation (2) and (3), the ^{14}C reservoir age offset in the Black Sea in 50 BP [i.e. $d^{14}R_{Black\ sea}(Y)$] was of 474±41 ^{14}C yr.

Although this approach can be applied to coral annual growth bands (e.g. Druffel et al., 2001), it is more generally used for museum collection samples (e.g. Siani et al., 2000; Tisnerat et al., 2010). The main limitation comes from the fact that collections have historical and scientific significance. Samples from museum collection may not always be available for destructive radiocarbon measurements. Furthermore few museum collections exist from prior to ca. AD 1700, limiting the temporal range. As well, these collections do not cover all the Earth's areas limiting the spatial range of reservoir age offset reconstruction. Finally, sometimes the information related to the date of entry in the collection may not match the year of death of the samples (for further information regarding limitations, see Ascough et al., 2005).

2.3. Reservoir age ^{14}C offset calculation based on a pair of ^{14}C age and weakly known calendar age

Things are more complicated when the calendar age θ for event Y is weakly known, i.e. that an uncertainty σ_θ is associated to θ. This arises when the calendar age was obtained from scientific measurements which could have been achieved through uranium-thorium dating for corals or speleothems (e.g. Durand et al., 2013; Southon et al., 2012) or by cross-matching between a sedimentary archive and a series of reference independently dated over the calendar time scale T (Bard et al., 2013; Heaton et al., 2013; Soulet et al., 2011a).

In this case for which, event Y has been dated to $\theta \pm \sigma_\theta$ in the calendar time space T, we would like to "uncalibrate" calendar age θ using the atmospheric calibration curve to obtain the corresponding atmosphere-derived ^{14}C age. A way to proceed would be to invert the axis of the calibration curve and to apply the regular calibration process. However, this is impossible since the calibration curve is built so that the ^{14}C time scale R function is a single valued continuum in the calendar time scale T but not vice-versa. Thus to get access to the atmospheric-derived ^{14}C age associated to event Y dated to $\theta \pm \sigma_\theta$, we propose to calibrate each ^{14}C age r of the ^{14}C time scale R and to evaluate the closeness of each resulting calibrated age distribution to the distribution of calendar age θ (**Fig. 1**).

In this scheme, the probability distribution of the measured calendar age for event Y given any calendar age t from the calendar time scale T can be represented by a normal distribution evaluated at t and centered on θ with a standard deviation σ_θ:

$$p(Y|t) \sim N(t; \theta, \sigma_\theta) \quad (4)$$

This can be written as:

$$p(Y|t) = \frac{1}{\sigma_\theta\sqrt{2\pi}} exp\left(-\frac{(t-\theta)^2}{2\sigma_\theta^2}\right) \quad (5)$$

This quantity evaluate the closeness between the occurrence of event Y and any time through the calendar age scale T. Additionally, we have information about how the ^{14}C and calendar time scales are related. The information comes from the atmospheric calibration curve which links the ^{14}C time scale R to the calendar time scale T. For any time t from the calendar time scale T, the atmospheric calibration curve is defined as $\rho(t) \pm \sigma(t)$ on the radiocarbon time scale R. Here $\rho(t)$ is the ^{14}C age of the atmosphere at calendar time t. For any age r from the ^{14}C time scale R, this information is normally taken to be:

$$p(r|t) \sim N\big(r; \rho(t), \sigma(t)\big) \quad (6)$$

This can be written as:

$$p(r|t) = \frac{1}{\sigma(t)\sqrt{2\pi}} exp\left(-\frac{\big(r-\rho(t)\big)^2}{2\sigma^2(t)}\right) \quad (7)$$

Now, let's assume the following Bayesian network: $Y \leftrightarrow T \rightarrow R$. In this network, the calendar time scale T is our hypothesis (or *prior*). Furthermore, we know that the radiocarbon time scale R depends upon the calendar time scale T (i.e. the calibration curve or the *model*) and we want to evaluate the closeness (or *likelihood*) between the calendar age measurement for event Y (our *observation*) and the calibration curve. According to the network and Bayes' theorem, we write:

$$p(Y|t,r) \propto p(Y|t) \cdot p(r|t) \cdot p(t) \quad (8)$$

The symbol $\propto$ denotes proportionality. The *prior* along the calendar time scale T is taken as uniform:

$$p(t) \sim U(-\infty, +\infty) \tag{9}$$

and is thus equal to a constant:

$$p(t) = constant \tag{10}$$

Thus according to equations (9) and (10), we say:

$$p(Y|t,r) \propto p(Y|t) \cdot p(r|t) \tag{11}$$

By substituting equations (5) and (7) in equation (11), we can rewrite as follows:

$$p(Y|t,r) \propto \frac{1}{\sigma_\theta \cdot \sigma(t)} exp\left(-\frac{(t-\theta)^2}{2\sigma_\theta^2}\right) \cdot exp\left(-\frac{\left(r-\rho(t)\right)^2}{2\sigma^2(t)}\right) \tag{12}$$

We now can integrate out parameter t:

$$p(Y|r) \propto \int p(Y|t) \cdot p(r|t) \cdot dt \tag{13}$$

The "uncalibrated" ^{14}C age (or *posterior*) defines the probability of obtaining a given ^{14}C age r from the radiocarbon time scale R given the event Y. From Bayes' theorem, the *posterior* is given by:

$$p(r|Y) \propto p(Y|r) \cdot p(r) \tag{14}$$

The *prior* along the radiocarbon time scale R is taken uniform. Thus $p(r)$ is constant and the probability distribution of the "uncalibrated" ^{14}C age (*posterior*) is the same as that for the *likelihood*:

$$p(r|Y) \propto p(Y|r) \tag{15}$$

Finally, to obtain the probability distribution of the atmospheric-derived ^{14}C age along the ^{14}C time scale R (i.e. the "uncalibrated" ^{14}C age) given the single event Y for which we know the calendar measurement $\theta \pm \sigma_\theta$, we normalize to 1. This gives:

$$p(r|Y)_{atm} = \frac{p(r|Y)}{\int p(r|Y) \cdot dr} \quad (16)$$

Here the denominator is the normalizing constant. The subscript "atm" on the left term of equation (16) stands to emphasize that this probability distribution is our atmospheric-derived ^{14}C age. At that step, we have "uncalibrated" our calendar age. Remember that event Y is characterized by both its calendar age and the ^{14}C age of the reservoir. We can write:

$$\rho_{atm}(Y) = p(r|Y)_{atm} \quad \text{and} \quad \rho_{res}(Y) = p(r|Y)_{res} \quad (17)$$

Now, according to equation (3), to find the probability distribution of the reservoir age offset which is $p(d^{14}R|Y)$, we have to subtract both quantities. Since both ^{14}C age distributions are independent, we use the convolution product:

$$p(d^{14}R|Y) = p(r|Y)_{res} * (-\mathbb{1}_R \cdot p(r|Y)_{atm}) \quad (18)$$

Here, $-\mathbb{1}_R$ means that we multiply by –1 the atmospheric-derived ^{14}C age along the ^{14}C time scale R before summing both probability distributions through the convolution product, and finally:

$$d^{14}R(Y) = p(d^{14}R|Y) \quad (19)$$

The *uncalibration-convolution process* fully propagates uncertainties linked to the reservoir-derived ^{14}C age and the calendar age of event Y, as well as the calibration curve wiggles and

uncertainties. **Fig. 1** shows that the both the uncalibrated ^{14}C age and the resulting reservoir age offset are not necessarily Gaussian in shape.

The *uncalibration-convolution process* developed here does not take into account any sedimentary ordering constraints that are available when dealing with high-resolution records of calendar observations. Ordering constraints can be incorporated in the calculations of reservoir age offset using some recent developments of the program OxCal (Bronk Ramsey et al., 2012; Bronk Ramsey and Lee, 2013).

2.4. The "ResAge" package: open-source codes for reservoir age offset calculations

Here, three codes for reservoir age offset calculation performing the above detailed three methodologies are provided (*ResAge* package). From data inputs (depending on the chosen approach), the codes provide the reservoir age ^{14}C offset outputs as well as some optional data.

Codes from the *ResAge* package have been written in the open-source environment R (R Development Core Team, 2014). R is freely downloadable at http://www.r-project.org for Windows, Mac and Linux. The codes make use of a command-window. The number of commands to be typed is extremely limited making very easy the use of these codes. Moreover, basics in R are relatively easy to learn, and the use of R in paleo-research has been growing recently (Blaauw, 2010; Blaauw and Christen, 2005, 2011; Haslett and Parnell, 2008; Heegaard et al., 2005). A manual containing information for installing and using the codes is also provided (see supplementary information).

Briefly, code "*rad2.r*" (say rad squared) is designed to calculate reservoir age offset when both the reservoir-derived and atmosphere-derived ^{14}C ages are known (see section 2.1). It returns a .csv file as output. Upon the user's decision, the atmospheric-derived ^{14}C ages can be calibrated.

255 An additional .csv file containing the calibrated density probabilities can be used to draw them.
256 A .txt file reports the unnormalized highest posterior probability as the confidence interval
257 specified by the user (see Blaauw, 2010).
258 Code "*colyear.r*" is designed for pairs of reservoir-derived ^{14}C age and perfectly known calendar
259 year (museum collection samples, coral annual band growths; see section 2.2). The code looks
260 up the calendar year in the atmospheric calibration curve, returns the corresponding atmosphere-
261 derives ^{14}C age and calculate the ^{14}C reservoir age offset. A .csv file is generated with all
262 information.
263 Code "*radcal.r*" is designed for pairs of reservoir-derived ^{14}C age and weakly-known calendar
264 age (e.g. ^{14}C and U/Th dating of corals and speleothem; see section 2.3). The calendar ages are
265 "uncalibrated" to obtain the corresponding atmosphere-derived ^{14}C age following the above
266 detailed procedure and ^{14}C reservoir age offsets are calculated through a convolution product.
267 Similar to Bronk Ramsey (2009b) and Blaauw (2010), calculations are performed in reference to
268 the ratio $F^{14}C$ (Reimer et al., 2004) instead of the ^{14}C age (Stuiver and Polach, 1977), allowing
269 for the best representation of all the ^{14}C uncertainties. Code returns a .csv file containing the ^{14}C
270 reservoir age offset density probabilities that can be used to draw them. A .txt file reports the
271 highest posterior probability as the confidence interval specified by the user. Upon user's request
272 the same information and files can be obtained for the "uncalibrated" atmospheric ^{14}C ages.

273

274 ## 3. A case study

275 Speleothems are promising archives to reconstruct past changes in the atmospheric ^{14}C
276 concentration. In 2013, three of these archives have been included for the first time in the
277 Intcal13 dataset in order to extend and refine the lastest release of the internationally ratified

atmospheric calibration curve (Intcal13; Reimer et al., 2013). Speleothems are secondary mineral deposits that precipitate from drip water in caves. They are mainly composed of calcite, aragonite and polymorphs of calcium carbonate and are considered as closed systems and thus suitable for ^{14}C measurements. Uranium from the groundwater is co-precipitated in calcite and aragonite with negligible thorium, making possible the use of U-Th dating methods and thus providing an independent calendar time scale. Accordingly, the three speleothem implemented in the Intcal13 dataset – two from the Bahamas (Beck et al., 2001; Hoffman et al., 2010) and one from China (Southon et al., 2012) – are dated through pairs of ^{14}C and U-Th ages. However, in the case of speleothems, obtained raw ^{14}C ages must be corrected for Dead Carbon Fraction (DCF) in order to estimate the "atmospheric equivalent" ^{14}C concentration. Indeed, DCF is the reservoir age offset between the speleothem and the atmosphere. DCF arises from the incorporation of a portion of ^{14}C-free inorganic carbon in the speleothem at the time of carbonate calcium precipitation (e.g. Fohlmeister et al., 2011; Genty and Massault, 1997). This portion of "dead" carbon is mainly due to dissolution of ^{14}C-free carbonate rocks overlying the cave.

As described in *Selection and Treatment of Data for ^{14}C Calibration* (Reimer et al., 2013b), DCF is estimated by analyzing a section of the speleothem that overlaps with the tree-ring-based section of the calibration curve (0-14,000 cal. a. BP in the Intcal13 lastest release). The mean ^{14}C offset between the ^{14}C age of the speleothem and the tree-ring-based portion of the calibration curve is then use as the DCF. An uncertainty term is then introduced. It quadratically takes into account the standard deviation of the individually calculated DCFs and the combined error of the ^{14}C measurement and of the inferred atmospheric ^{14}C related to the calibration curve (Reimer et al., 2013a, 2013b; Southon et al., 2012). In this approach, uncertainty in the U/Th ages and the wiggles of the calibration curve are not taken into account.

Here, the DCFs of the three speleothem-datasets [Hulu Cave H82 speleothem (Southon et al., 2012) and Bahamas speleothems GP89-24-1 and GP89-25-3 (Beck et al., 2001; Hoffmann et al., 2010, respectively)] for data overlapping the tree-ring based calibration curve are calculated applying the methodology detailed in section 2.3 through the use of the function *radcal* described in section 2.4).

Depending upon the number of data to be processed and on the uncertainty linked to the calendar U/Th age, calculations take up few seconds on a modern PC: ~5 sec for the 80 Hulu Cave data (mean $\sigma_{U/Th}$ of 30 yrs), ~7 sec for the 63 GP89-24-1 data (mean $\sigma_{U/Th}$ of 40 yrs) and ~20 sec for the 116 GP89-25-3 data (mean $\sigma_{U/Th}$ of 45 yrs).

Calculated DCFs for Hulu Cave H82 show no noticeable structures with limited variability with time – 95%-confidence interval of 308 to 615 ^{14}C years with a mode (highest probability) at 433 ^{14}C years (**Fig. 2**). DCF variability for both Bahamas speleothem is considerably larger - 95%-confidence interval 1045 to 2099 ^{14}C years with a mode at 1405 ^{14}C years for GP89-24-1 speleothem (Beck et al., 2001) and 95%-confidence interval 1527 to 2755 ^{14}C years with a mode at 2124 ^{14}C years for GP89-25-3 speleothem (Hoffmann et al., 2010) (**Fig. 2**). Perhaps, a problematic feature is the marked structure seen in GP89-25-3 speleothem (Hoffmann et al., 2010) showing fast and high-amplitude changes in the DCF. As an example, between *c.* 12,200 and 11,900 cal. a. BP, DCF decreases by 1200 ^{14}C years. GP89-25-3 speleothem data are invaluable data that are currently used as input data to reconstruct the atmospheric ^{14}C calibration curve (Reimer et al., 2013a, 2013b). However, even corrected for a wide average DCF, such a structure occurring in older part of the speleothem record may introduce uncertainties by an order of 1000 cal. years for the older portion of the atmospheric ^{14}C calibration curve. Most of all, further developing our understanding of the controls on the incorporation of dead carbon in

speleothems (e.g. Fohlmeister et al., 2011; Noronha et al., 2014; Reimer et al., 2013b) and in a general manner on the reservoir age offset of the marine data implemented in the ^{14}C calibration curve are both of primary interest (Reimer et al., 2013b).

4. Conclusions

Proper calculation of reservoir age offset is of primary interest since their reconstruction through time tells a lot about the changes in the regional to global-scale carbon cycle with impacts on our understanding of the Earth climate. In particular, proper regional reconstruction of reservoir age offsets is important to build regional calibration curve. Regional calibration curves may be suitable for very specific basins (e.g. Black Sea, Caspian Sea) for which reservoir offsets are supposed to have greatly varied with time and for which assessing reliable sediment archive chronologies is challenging (e.g. Kwiecien et al., 2008; Soulet et al., 2011a, 2011b). Regional surface ocean calibration curves are also needed to better constrain changes in the oceanic ventilation age through the projection age methods (Lund, 2013). R codes and the innovative calculation method based on pairs of ^{14}C age and calendar ages presented here would represent another step to study reservoir age offset evolution with more scrutiny. Future improvements and development aiming at properly calculating the reservoir age offset evolution with time would be useful. Finally, the R codes composing the *ResAge* package can be understood relatively easily. Interested users can open and adapt the "black box".

References:

Ascough, P., Cook, G., Dugmore, A., 2005. Methodological approaches to determining the marine radiocarbon reservoir effect. Progress in Physical Geography, 29(4), 532-547.

Bard, E., Arnold, M., Mangerud, J., Paterne, M., Labeyrie, L., Duprat, J., Mélières, M.-A., Sønstegaard, E., Duplessy, J. C., 1994. The North Atlantic atmosphere-sea surface ^{14}C gradient during the Younger Dryas climatic event. Earth and Planetary Science Letters, 126(4), 275-287.

Bard, E., Ménot, G., Rostek, F., Licari, L., Böning, P., Edwards, R.L., Cheng, H., Wang, Y., Heaton, T.J., 2013. Radiocarbon calibration/comparison records based on marine sediments from the Pakistan and Iberian margins. Radiocarbon, 55(4), 1999-2019.

Beck, J.W., Richards, D.A., Lawrence, R., Silverman, B.W., Smart, P.L., Donahue, D.J., Hererra-Osterheld, S., Burr, G.S., Calsoyas, L., Jull, A.J.T., Biddulph, D., 2001. Extremely large variations of atmospheric ^{14}C concentration during the last glacial period. Science, 292(5526), 2453-2458.

Blaauw, M., 2010. Methods and code for 'classical'age-modelling of radiocarbon sequences. Quaternary Geochronology, 5(5), 512-518.

Blaauw, M., Christen, J.A., 2005. Radiocarbon peat chronologies and environmental change. Applied Statistics 54, 805-816.

Blaauw, M., Christen, J.A., 2011. Flexible paleoclimate age-depth models using an autoregressive gamma process. Bayesian Analysis, 6(3), 457-474.

Bondevik, S., Birks, H.H., Gulliksen, S., Mangerud, J., 1999. Late Weichselian Marine ^{14}C Reservoir Ages at the Western Coast of Norway. Quaternary Research, 52(1), 104-114.

Bondevik, S., Mangerud, J., Birks, H.H., Gulliksen, S., Reimer, P., 2006. Changes in North Atlantic radiocarbon reservoir ages during the Allerød and Younger Dryas. Science, 312(5779), 1514-1517.

Bronk Ramsey, C., 2008. Deposition models for chronological records. Quaternary Science Reviews, 27, 42-60.

Bronk Ramsey, C., 2009a. Dealing with outliers and offsets in radiocarbon dating. Radiocarbon, 51(3), 1023-1045.

Bronk Ramsey, C., 2009b. Bayesian analysis of radiocarbon dates. Radiocarbon, 51(1), 337-360.

Bronk Ramsey, C., Lee, S., 2013. Recent and planned developments of the program OxCal. Radiocarbon, 55(2–3), 720-730.

Ramsey, C.B., Staff, R.A., Bryant, C.L., Brock, F., Kitagawa, H., van der Plicht, J., Schlolaut, G., Marshall, M.H., Brauer, A., Lamb, H.F., Payne, R.L., Tarasov, P.E., Haraguchi, T., Gotanda, K., Yonenobu, H., Yokoyama, Y., Tada, R., Nakagawa, T. (2012). A complete terrestrial radiocarbon record for 11.2 to 52.8 kyr BP. Science, 338(6105), 370-374.

Druffel, E.R., Griffin, S., Guilderson, T.P., Kashgarian, M., Southon, J., Schrag, D.P., 2001. Changes of subtropical North Pacific radiocarbon andcorrelation with climate variability. Radiocarbon, 43(1), 15-25.

Druffel, E.R., Robinson, L.F., Griffin, S., Halley, R.B., Southon, J.R., Adkins, J.F., 2008. Low reservoir ages for the surface ocean from mid-Holocene Florida corals. Paleoceanography, 23(2), PA2209. doi: 10.1029/2007PA001527.

Durand, N., Deschamps, P., Bard, E., Hamelin, B., Camoin, G., Thomas, A.L., Henderson, G.H., Yokoyama, Y., Matsuzaki, H., 2013. Comparison of ^{14}C and U-Th ages in corals from IODP #310 cores offshore Tahiti. Radiocarbon, 55(4), 1947-1974.

Fohlmeister, J., Kromer, B., Mangini, A., 2011. The influence of soil organic matter age spectrum on the reconstruction of atmospheric ^{14}C levels via stalagmites. Radiocarbon, 53(1), 99-115.

Gentil, D., Massault, M., 1997. Bomb 14C recorded in laminated speleothems: calculation of dead carbon proportion. Radiocarbon 33(1):33–48.

Hall, B.L., Henderson, G.M., Baroni, C., Kellogg, T.B., 2010. Constant Holocene Southern-Ocean ^{14}C reservoir ages and ice-shelf flow rates. Earth and Planetary Science Letters 296(1), 115-123.

Haslett, J., Parnell, A., 2008. A simple monotone process with application to radiocarbon-dated depth chronologies. Applied Statistics 57, 1-20.

Heaton, T.J., Bard, E., and Hughen, K.A., 2013. Elastic Tie-Pointing—Transferring Chronologies between Records Via a Gaussian Process. Radiocarbon 55(4), 1975-1997.

Heegaard, E., Birks, H.J.B., Telford, R.J., 2005. Relationships between calibrated ages and depth in stratigraphical sequences: an estimation procedure by mixed effect regression. The Holocene 15, 1-7.

401 Hoffmann, D.L., Beck, J.W., Richards, D.A., Smart, P.L., Singarayer, J.S., Ketchmark, T. Hawkesworth,
402 C.J., 2010. Towards radiocarbon calibration beyond 28ka using speleothems from the Bahamas.
403 Earth and Planetary Science Letters, 289(1), 1-10.

404 Hogg, A. G., Hua, Q., Blackwell, P. G., Niu, M., Buck, C. E., Guilderson, T. P., Heaton, T. J., Palmer, J.
405 G., Reimer, P. J., Reimer, R. W., Turney, C. S. M., and Zimmerman, S. R. H., 2013. SHCal13
406 Southern Hemisphere calibration, 0–50,000 years cal BP. Radiocarbon, 55(4), 1889-1903.

407 Jones M, Nicholls G., 2001. Reservoir offset models for radiocarbon calibration. Radiocarbon, 43(1),
408 119–24.

409 Jones M, Petchey F, Green R, Sheppard P, Phelan M., 2007. The marine ΔR for Nenumbo (Solomon
410 Islands): a case studying calculating reservoir offsets from paired sample data. Radiocarbon,
411 49(1), 95–102.

412 Jull, A. J., Burr, G.S., Hodgins, G.W., 2013. Radiocarbon dating, reservoir effects, and calibration.
413 Quaternary International 299, 64-71.

414 Kwiecien, O., Arz, H.W., Lamy, F., Wulf, S., Bahr, A., Rohl, U., Haug, G.H., 2008. Estimated reservoir
415 ages of the Black Sea since the last glacial. Radiocarbon, 50(1), 99.

416 Lund, D.C., 2013. Deep Pacific ventilation ages during the last deglaciation: Evaluating the influence of
417 diffusive mixing and source region reservoir age. Earth and Planetary Science Letters, 381, 52-
418 62.

419 Noronha, A.L., Johnson, K.R., Hu, C., Ruan, J., Southon, J.R., Ferguson, J.E., 2014. Assessing influences
420 on speleothem dead carbon variability over the Holocene: Implications for speleothem-based
421 radiocarbon calibration. Earth and Planetary Science Letters, 394, 20-29.

422 R Core Team, 2014. R: A Language and Environment for Statistical Computing. R Foundation for
423 Statistical Computing, http://www.R-project.org.

424 Reimer, P.J., Bard, E., Bayliss, A., Beck, J.W., Blackwell, P.G., Bronk Ramsey, C., Buck, C.E., Cheng,
425 H., Edwards, R.L., Friedrich, M., Grootes, P.M., Guilderson, T.P., Haflidason, H., Hajdas, I.,
426 Hatté, C., Heaton, T.J., Hoffmann, D.L., Hogg, A.G., Hughen, K.A., Kaiser, K.F., Kromer, B.,
427 Manning, S.W., Niu, M., Reimer, R.W., Richards, D.A., Scott, E.M., Southon, J.R., Staff, R.A.,
428 Turney, C.S.M., and van der Plicht, J., 2013a. IntCal13 and Marine13 Radiocarbon Age
429 Calibration Curves 0–50,000 Years cal BP. Radiocarbon 55(4), 1869-1887.

Reimer, P.J., Bard, E., Bayliss, A., Beck, J.W., Blackwell, P.G., Ramsey, C.B., Brown, D.M., Buck, C.E., Edwards, R.L., Friedrich, M., Grootes, P.M., Guilderson, T.P., Haflidason, H., Hajdas, I., Hatté, C., Heaton, T.J., Hogg, A.G., Hughen, K.A., Kaiser, K.F., Kromer., B., Manning, S.W., Reimer, R.W., Richards, D.A., Scott, E.M., Southon, J.R., Turney, C.S.M., van der Plicht, J., 2013b. Selection and treatment of data for radiocarbon calibration: an update to the International Calibration (IntCal) criteria. Radiocarbon, 55(4), 1923-1945.

Reimer, P.J., Brown, T.A., Reimer, R.W, 2004. Discussion: reporting and calibration of post-bomb ^{14}C data. Radiocarbon, 46(3), 1299-1304.

Siani, G., Michel, E., De Pol-Holz, R., DeVries, T., Lamy, F., Carel, M., Isguder, G., Dewilde, F., Lourantou, A., 2013. Carbon isotope records reveal precise timing of enhanced Southern Ocean upwelling during the last deglaciation. Nature communications, 4. doi: 10.1038/ncomms3758.

Siani, G., Paterne, M., Arnold, M., Bard, E., Mativier, B., Tisnerat, N., Bassinot, F., 2000. Radiocarbon reservoir ages in the Mediterranean Sea and Black Sea. Radiocarbon, 42(2), 271-280.

Siani, G., Paterne, M., Michel, E., Sulpizio, R., Sbrana, A., Arnold, M., Haddad, G., 2001. Mediterranean Sea surface radiocarbon reservoir age changes since the last glacial maximum. Science, 294(5548), 1917-1920.

Soulet, G., Ménot, G., Garreta, V., Rostek, F., Zaragosi, S., Lericolais, G., Bard, E., 2011a. Black Sea "Lake" reservoir age evolution since the Last Glacial - Hydrologic and climatic implications. Earth and Planetary Science Letters 308, 245-258.

Soulet, G., Ménot, G., Lericolais, G., Bard, E., 2011b. A revised calendar age for the last reconnection of the Black Sea to the global ocean. Quaternary Science Reviews, 30(9), 1019-1026.

Southon, J., Mohtadi, M., De Pol-Holz, R., 2013. Planktonic foram dates from the Indonesian Arc: marine ^{14}C reservoir ages and a mythical AD 535 eruption of Krakatau. Radiocarbon, 55(2-3), 1164-1172.

Southon, J., Noronha, A.L., Cheng, H., Edwards, R.L., Wang, Y., 2012. A high-resolution record of atmospheric ^{14}C based on Hulu Cave speleothem H82. Quaternary Science Reviews 33**,** 32-41.

Southon, J., Noronha, A.L., Cheng, H., Edwards, R.L., Wang, Y., 2012. A high-resolution record of atmospheric ^{14}C based on Hulu Cave speleothem H82. Quaternary Science Reviews, 33, 32-41.

Stuiver, M., Polach, H.A., 1977. Discussion: reporting of ^{14}C data. Radiocarbon, 19(3), 355-363.

Thornalley, D.J.R., Barker, S., Broecker, W.S., Elderfield, H., McCave, I.N., 2011. The Deglacial Evolution of North Atlantic Deep Convection. Science 331(6014), 202-205.

Tisnérat-Laborde, N., Paterne, M., Métivier, B., Arnold, M., Yiou, P., Blamart, D., Raynaud, S., 2010. Variability of the northeast Atlantic sea surface $\Delta^{14}C$ and marine reservoir age and the North Atlantic Oscillation (NAO). Quaternary Science Reviews, 29(19), 2633-2646.

Acknowledgements: G.S. acknowledges the Postdoctoral Scholar Program at the Woods Hole Oceanographic Institution (WHOI), with funding provided by the National Ocean Sciences Accelerator Mass Spectrometry Facility (NOSAMS). G.S. warmly thanks Beatrice Tomasi, William J. Jenkins, Steven R. Beaupré, Ann P. McNichol, Kirstyn Fornace, Liviu Giosan and Valier Galy for fruitful discussions and support.

Figure captions:

Fig. 1: Calculation of a ^{14}C reservoir age offset based on a pair of reservoir-derived ^{14}C date of 9200 ± 30 ^{14}C yr BP (grey Gaussian probability density function [pdf] on the radiocarbon time axis) and calendar date of 9550 ± 150 cal. yr BP (light green Gaussian pdf on the calendar time axis). A: "Uncalibration" of the calendar date following the methodology detailed in section 2.3. The resulting "uncalibrated" age (light green multimodal pdf on the radiocarbon time axis) corresponds to the atmosphere-derived ^{14}C age involved in the ^{14}C reservoir age offset calculation. Highest posterior density ranges (black bars) of the "uncalibrated" age are 8272 – 8601 ^{14}C yr BP (probability 43.8%) and 8605 – 8826 ^{14}C yr BP (probability 51.2%). Black curve

482 is the 1σ Intcal13 envelope (Reimer et al., 2013). B: The resulting ^{14}C reservoir age offset
483 (purple pdf) corresponding to the difference between the reservoir-derived ^{14}C age (grey
484 Gaussian pdf in A) and the atmosphere-derived ^{14}C age (light green multimodal pdf in A)
485 through a convolution product. Highest posterior density ranges (black bars) of the ^{14}C reservoir
486 age offset are 362 – 617 ^{14}C years (probability 51.9%) and 622 – 947 ^{14}C years (probability
487 43.1%).
488
489 **Fig. 2**: Reconstruction of the changes in the ^{14}C reservoir age offset (i.e. dead carbon fraction,
490 DCF) for the three speleothem data currently included in the Intcal13 database. DCF is
491 calculated for ^{14}C-calendar pairs overlapping the tree-ring based atmospheric calibration curve
492 (Intcal13; Reimer et al., 2013). Yellow and green squares: Bahamas speleothems GP89-25-3
493 (Hoffmann et al., 2010) and GP89-24-1 (Beck et al., 2001), respectively. Blue circles: Chinese
494 Hulu Cave speleothem H82 (Southon et al., 2012). Yellow, green and blue probability density
495 functions (pdf) represent the corresponding full variability in the DCF calculated as the mixture
496 of all the individual DCF pdfs for each set of data: Highest posterior density ranges at 95%
497 (shaded areas) and modes are 1527 – 2755 ^{14}C years with mode at 2124 ^{14}C years (Bahamas
498 GP89-25-3), 1045 – 2099 ^{14}C years with mode at 1405 ^{14}C years (Bahamas GP89-24-1) and 308
499 – 615 ^{14}C years with mode at 433 ^{14}C years (Chinese Hulu cave H82). All uncertainties
500 characterizing data are given at 95% confidence.

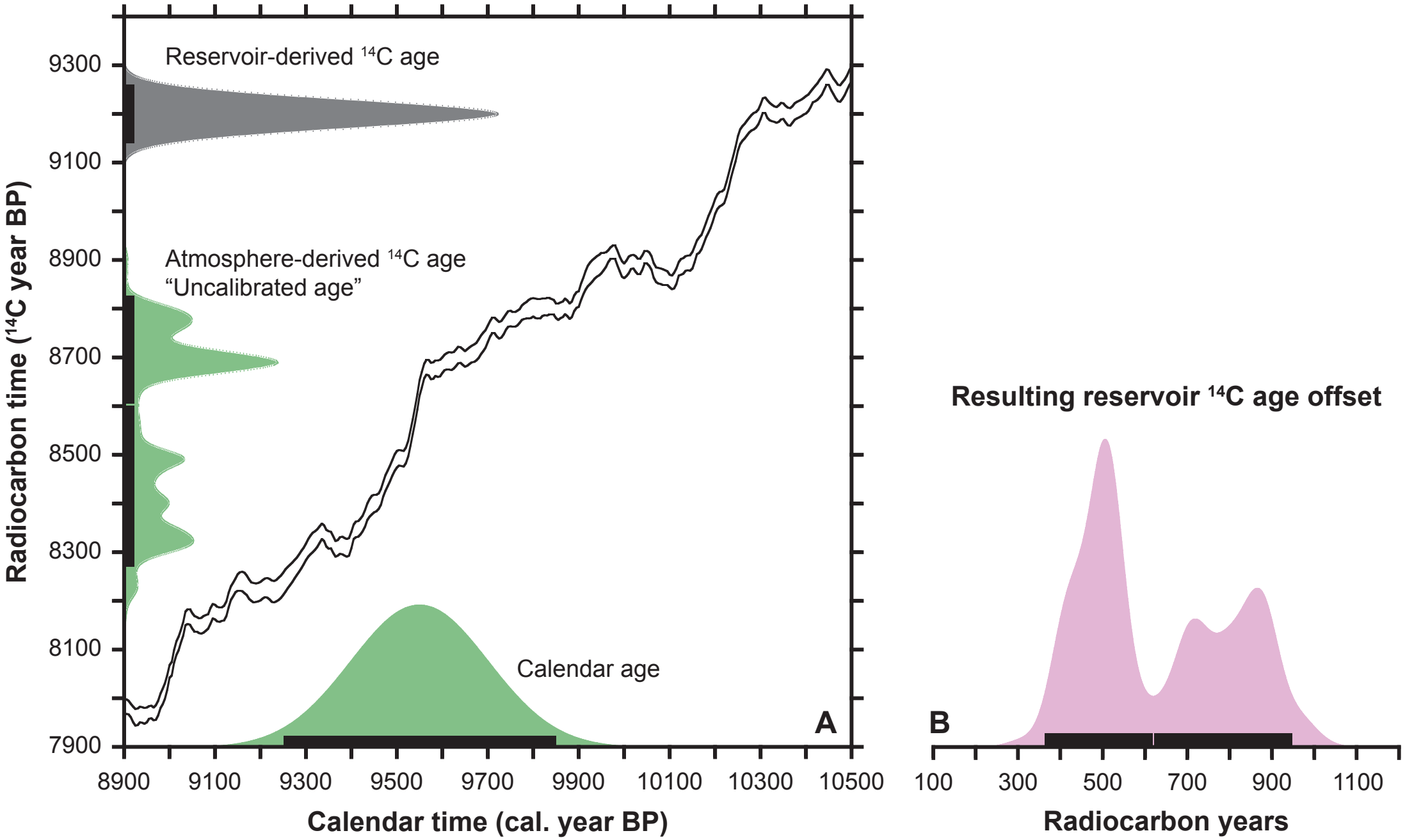
Reservoir-derived ^{14}C age
Atmosphere-derived ^{14}C age
"Uncalibrated age"
Calendar age
A
B
Radiocarbon time (^{14}C year BP)
Calendar time (cal. year BP)
Resulting reservoir ^{14}C age offset
Radiocarbon years
9300
9100
8900
8700
8500
8300
8100
7900
8900
9100
9300
9500
9700
9900
10100
10300
10500
100
300
500
700
900
1100

Figure 1.

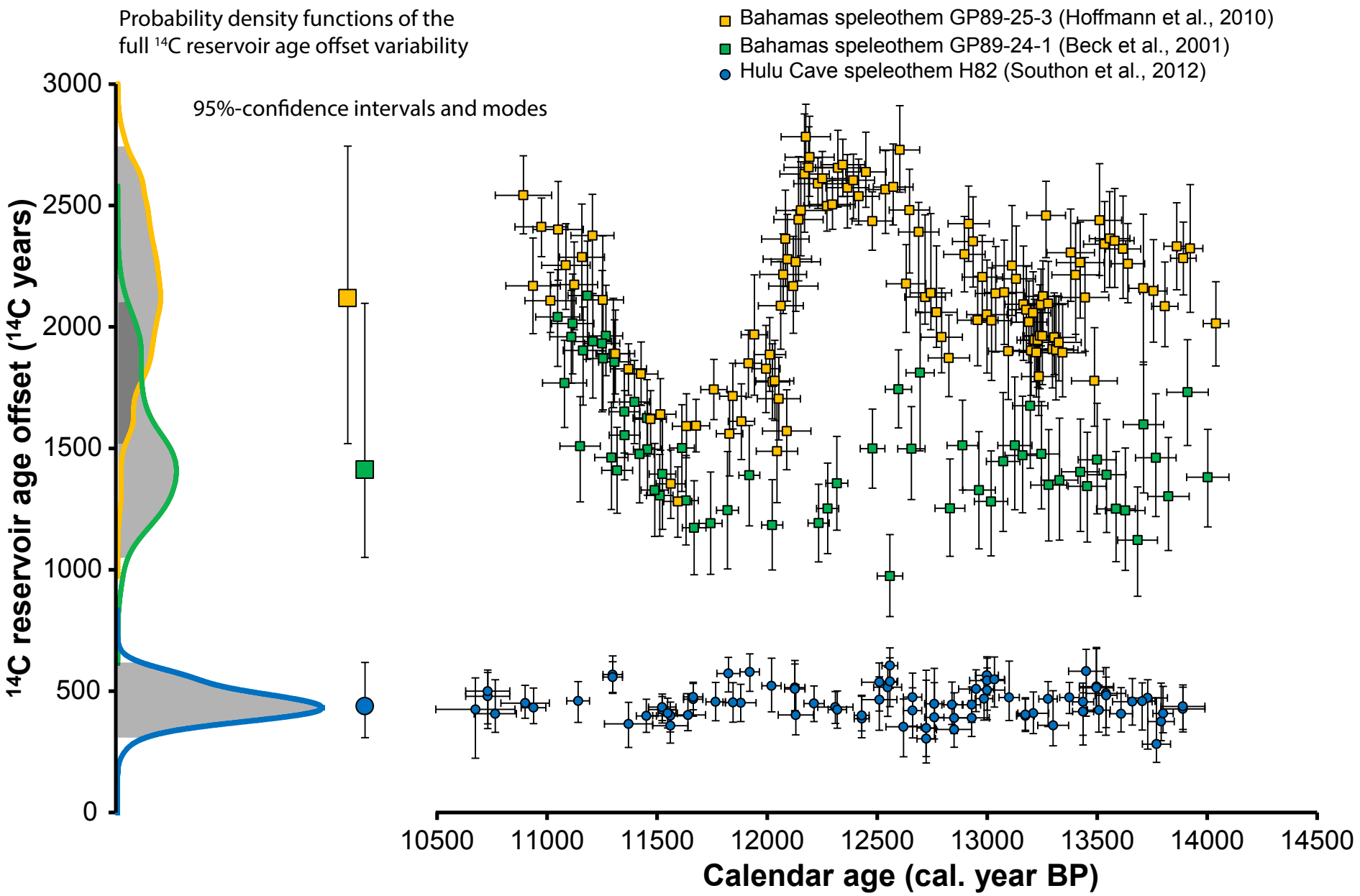
Probability density functions of the
full ¹⁴C reservoir age offset variability
95%-confidence intervals and modes
Bahamas speleothem GP89-25-3 (Hoffmann et al., 2010)
Bahamas speleothem GP89-24-1 (Beck et al., 2001)
Hulu Cave speleothem H82 (Southon et al., 2012)
¹⁴C reservoir age offset (¹⁴C years)
3000
2500
2000
1500
1000
500
0
10500
11000
11500
12000
12500
13000
13500
14000
14500
Calendar age (cal. year BP)

Figure 2.